

Original Article

## A performance investigation of a multi-staging hydrokinetic turbine for river flow



Kerishmaa Theavy Kunalan, Ng Cheng Yee\* , Maldar Nauman Riyaz

Department of Civil and Environmental Engineering, Universiti Teknologi PETRONAS, Seri Iskandar 32610, Perak, Malaysia

### Abstract

Our world has been relying on fossil fuel, non-renewable energy, that is depleting day by day and negatively impacting the environment. Hydropower is known to contribute a significant portion of the renewable power production. Dams have been the most common technique to generate hydropower. However, such a scheme was not able to support the rural areas as it requires large areas and a huge amount of water resource. Savonius hydrokinetic turbine (HKT) has been suggested as the device for a small-scale application as it can generate power from low-velocity river flow with less installation cost. With that, the aim of this study is designed to investigate and compare the performance of the single-staged and two-staged HKT for river flow. This study considered numerical simulation that includes modeling, testing, and analyzing the data. Then, comparing it with the existing literature results, to identify the solution. This investigation demonstrates an improvement of 8.1% in the efficiency of power coefficient when compared with single-staged HKT.

Copyright © 2021 PENERBIT AKADEMI BARU - All rights reserved

### Article Info

Received 5 June 2021

Received in revised form 26 December 2021

Accepted 31 December 2021

Available online 3 January 2022

### Keywords

Savonius turbine

Two-staged hydrokinetic turbine

Tip speed ratio

## 1 Introduction

Renewable Energy is derived from natural resources that are constantly replenished, and it is supplied on human timescales. This energy is usually utilized in areas such as power generation, transportation, heating, etc. Renewable energy sources are gaining interest as they are less expensive and readily available [1]. Besides, it can provide better health for the community, since the reduction of fossil fuels consumption is expected to improve the global warming and climate change scenario. Furthermore, the generation of energy from renewables produces no greenhouse gas (GHG) emissions and helps to reduce air pollution. It has been recorded that the global emissions of GHG rose about 1.7% in 2018 to a record of more than 33 billion tonnes, as energy demand grew by 2.3% [2].

The most common types of renewable energy sources include solar, wind, biomass, hydro, and geothermal. Of all these energy sources, hydropower is reported to be the most preferable due to distinct advantages such as high power density and predictability [3]. Hydropower plants can be classified into conventional and unconventional systems. The conventional system is based on extracting the potential energy of falling water and converting it to electricity. It requires huge structures such as dams or reservoirs that are constructed at a higher ground level to facilitate water storage. However, reports have mentioned that the major disadvantage of this system is the irreversible damage it causes to the environment as well as the disruption to the ecosystem of aquatic life [4]. Besides, it has a limitation that it is unable to extract energy from ocean currents or low-velocity stream flows [5].

\* Corresponding author [chengyee.ng@utp.edu.my](mailto:chengyee.ng@utp.edu.my) ✉

The unconventional system refers to the hydrokinetic turbine (HKT). In general, HKTs do not require any large amount of water storage like in the case of dams. The kinetic energy from the free-flowing streams such as rivers or oceans is converted into electricity through the rotation of the HKT blades [6]. Basically, there are two categories of HKTs that differ in orientation with regards to incoming flow i.e., the horizontal axis HKT and vertical axis HKT. Amongst the various designs of HKTs, the Savonius turbine has been reported to be able to initiate self-starting and generate high torque at relatively low flow speeds [7]. Hence, the Savonius turbine has been focused herein for this study. The Savonius turbine was originally invented by Finish engineer Sigurd J. Savonius in 1920 for wind energy applications. It is a drag-based energy conversion device and its blades resemble the shape of the letter “S” as shown in Fig. 1 [8].

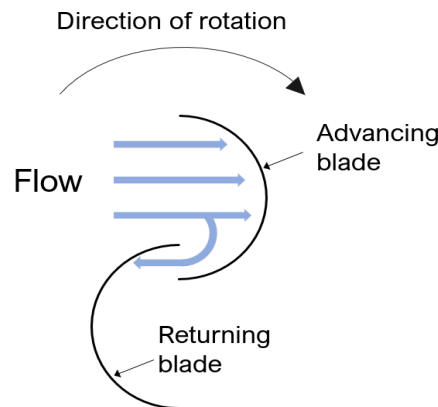


**Fig. 1** Top view of conventional Savonius rotor [9]

Compared to the convex, the concave surface results in a higher drag coefficient which facilitates the rotation of the turbine. The high-strength blades give a greater starting torque to the turbine compared with low-solidity blades at the same force applied from the river [10]. A power curve is normally used to rate the HKT operation, which is represented in terms of the power coefficient ( $C_p$ ) as a function of tip-speed ratio (TSR). The Betz limits of 0.539, which represents the maximum  $C_p$  of any HKT can reach when the HKT operates in an unconstrained flow [11]. Fig. 2 shows the power curves for different types of turbines [12]. To summarize, the vertical-axis HKT systems perform better at lower TSR or low-velocity flows that are typically less than 1.0 m/s with shallow depths. However, the vertical-axis HKTs have lower power harnessing efficiency compared to the horizontal ones. Nevertheless, the allowable reduction in size for the vertical axis HKTs owing to the possible extension along the width of the channel allows them to be installed in small areas such as shallow river flows. Even though Savonius hydrokinetic turbine (SHT) is considered useful, it is not as commercially acknowledged as the other types of HKTs. Yet, numerous researchers have claimed it to be an appropriate option for power generation from low-velocity river flows [7].

## 2 Techniques of improving the Savonius Hydrokinetic Turbine performances

As mentioned earlier, the performance of Savonius turbine is not as efficient as the other types. This leaves an ample room for performance improvement which can be achieved through modifications in its structural design. Over the years, several different techniques have been studied to improve the performance of the Savonius turbine [14]. In this study, we adopt a combination of two techniques i.e., multi-staged rotor arrangement and blade profile modification. The multi-staged assembly of the Savonius turbine involves placing the rotors one over another on a common central shaft and separated by an endplate. The rotors may have a phase angle orientation of either  $0^\circ$ ,  $90^\circ$ , or  $120^\circ$  depending upon the selected arrangement as shown in Fig. 3 [15].

The two-stage and three-stage arrangements have been the most commonly studied techniques in the available literature on multi-staged Savonius turbine. An experimental study was carried out by Nakajima et al. [16] for the multi-staged HKT. The results revealed that the  $C_p$  value of Savonius turbine

enhanced by 10% with the use of the two-staged configuration having a  $90^\circ$  phase difference between the blades. In another study conducted by Khan et al. [17], the authors found that the two-staged turbine provides better performances compared to the single and triple-staged. The maximum  $C_p$  value for single, two, and triple-staged Savonius HKT were reported to be 0.038, 0.049, and 0.040, respectively. Table 1 summarizes the optimization studies by researchers on multi-staged Savonius HKTs and their respective findings.

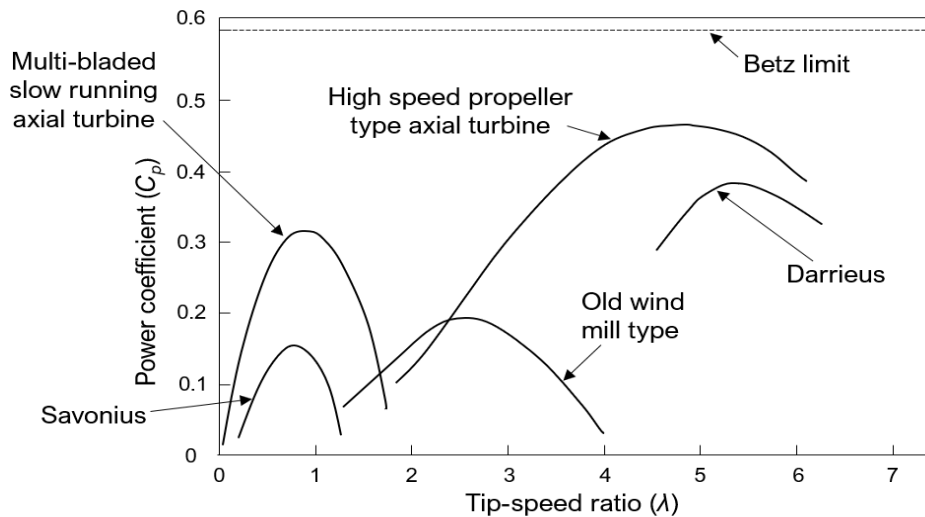


**Fig. 2** Betz limits graph [13]

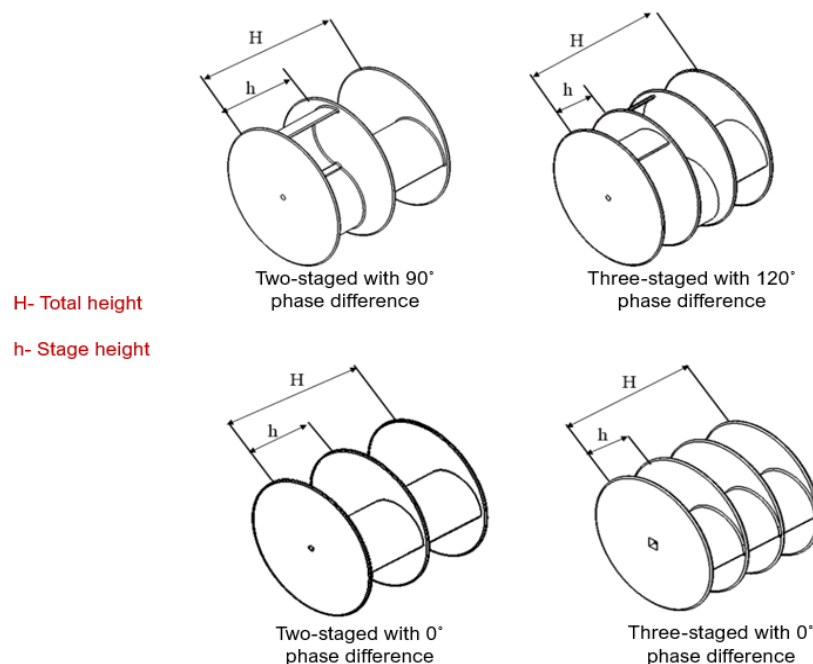


**Fig. 3** Multi-staged Savonius Hydrokinetic Turbine [15]

The blade profile modification involves altering the semi-circular blade shape of the conventional Savonius turbine in order to amplify the drag force exerted by the fluid on the concave surface facing the flow [25]. At the same time, emphasis is also given on decreasing the drag effect on the convex surface of the returning blade. The blade profile selected for the present study is a modified Bach blade profile which is selected on the basis of a recent investigation by Roy and Saha [26]. This type of Bach

blade design is composed by a straight line with an arc, as shown in Fig. 4. Roy and Saha tested different types of blade profiles which included the conventional semi-circular blades, semi-elliptic blades, Benesh type blades and the modified Bach profile. Based on their findings, the modified Bach profile recorded a  $C_{pmax}$  of 0.30 which was relatively greater than the other three aforementioned blade designs. The authors concluded that the modified Bach blade is able to demonstrate an improvement not only in terms of power coefficient, but also the torque coefficients and aerodynamic characteristics were better as compared to the conventional SHT.

**Table 1** Two stage as the optimization of the Savonius hydrokinetic turbine studies

Types of Energy	Title	Findings
Wind	A two-step Savonius rotor for local production of electricity: a design study [18]	The two-staged prototype delivered max power output of 120W
Wind	Optimum design configuration of Savonius rotor through wind tunnel experiments [19]	Experimental maximum power coefficient ( $C_{pmax}$ ) for two-staged rotor was 0.21
Water	Performance of Savonius Rotor as a Water Current Turbine [17]	Experimental $C_{pmax}$ obtained was 0.049
Water	Influence of the deflector plate on the performance of modified Savonius water turbine (90° phase with deflector plate) [20]	Experimental $C_{pmax}$ of 0.17 at a TSR of 0.83
Water	Experimental Studies on Savonius-type Vertical Axis Turbine for Low Marine Current Velocity [21]	Experimental $C_{pmax} = 0.14$
Wind	Performance Measurement of a two-staged two-bladed Savonius Rotor [22]	Experimental $C_{pmax} = 0.438$ at a TSR = 0.698
Wind	Numerical and experimental characterization of multi-stage Savonius rotors [23]	Experimental & numerical $C_{pmax}$ achieved = 0.081
Wind	Numerical and experimental study of a helical Savonius wind turbine and a comparison with a two-stage Savonius turbine [24]	The two-staged HKT achieved an experimental $C_{pmax}$ of 0.128 at TSR = 0.655

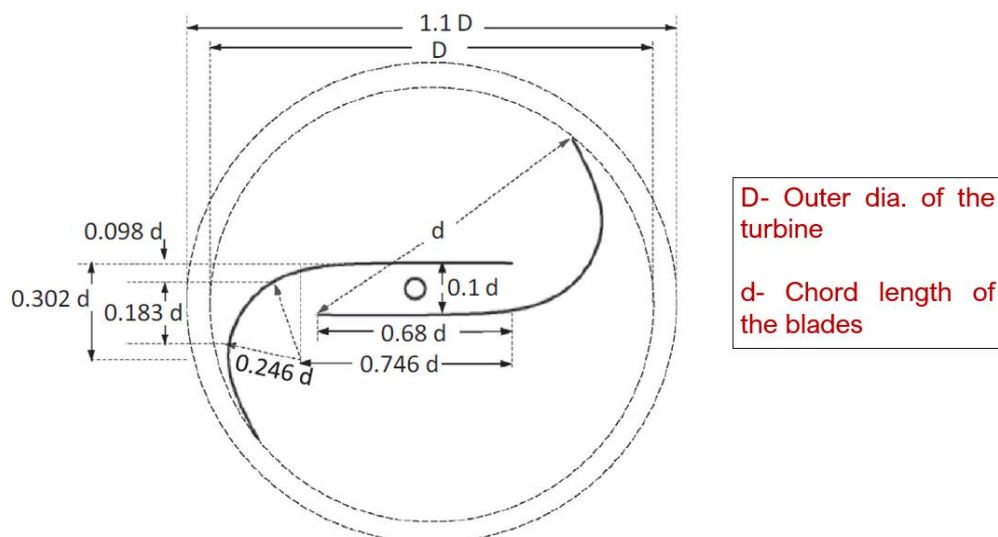


**Fig. 4** Modified Bach Blade Profile [26]

### 3 Methodology

The Savonius models used for the study are designed using the ANSYS Modeler software. The models are then processed into the Flow-3D software for the 3D simulation work. For any CFD study, it is extremely important to achieve validation with experimental results in order to demonstrate reliability of the obtained results. For the validation purposes, the simulation results were compared with the findings from Roy & Saha [26] for the parameters such as power coefficient ( $C_p$ ) and torque coefficient ( $C_t$ ). The referred study involves testing at different values of Reynolds number ( $Re$ ). For the purpose of validation, the single-staged Savonius turbine with modified Bach type blades has been simulated at an  $Re$  value of  $1.5 \times 10^5$  and the obtained results are compared with the experimental findings of Roy and Saha. The validated results are then followed up with modelling of two-staged Savonius HKT with modified Bach type blades. The simulations are repeated with Flow-3D software, and the results are analyzed and compared.

#### 3.1 Geometric parameters

The two different models- single-staged modified Bach and two-staged modified Bach as modeled in the Design Modeler software are shown in Fig. 5. Since the validation part of this study is based on the experimental results of Roy and Saha, similar value of aspect ratio equal to 1, has been maintained for the designed models. The aspect ratio is defined as the overall diameter ( $D$ ) to the total height ( $H$ ). To arrive at the optimum performance, it is necessary to control this parameter. For achieving an aspect ratio of 1, a same value of 191 mm is specified for both  $D$  as well as  $H$ .

The end plate is used at the top and bottom of the blades with a thickness of 4 mm and the internal blade diameter ( $D_o$ ) is 174 mm for both the simulated models. In case of two-staged model, the height for every stage ( $h_s$ ) is calculated to be 95.5 mm. Furthermore, based on the results reported from number of studies in the literature, a phase difference of  $90^\circ$  is adopted between both the stages of the two-staged modified Bach turbine [27–29].

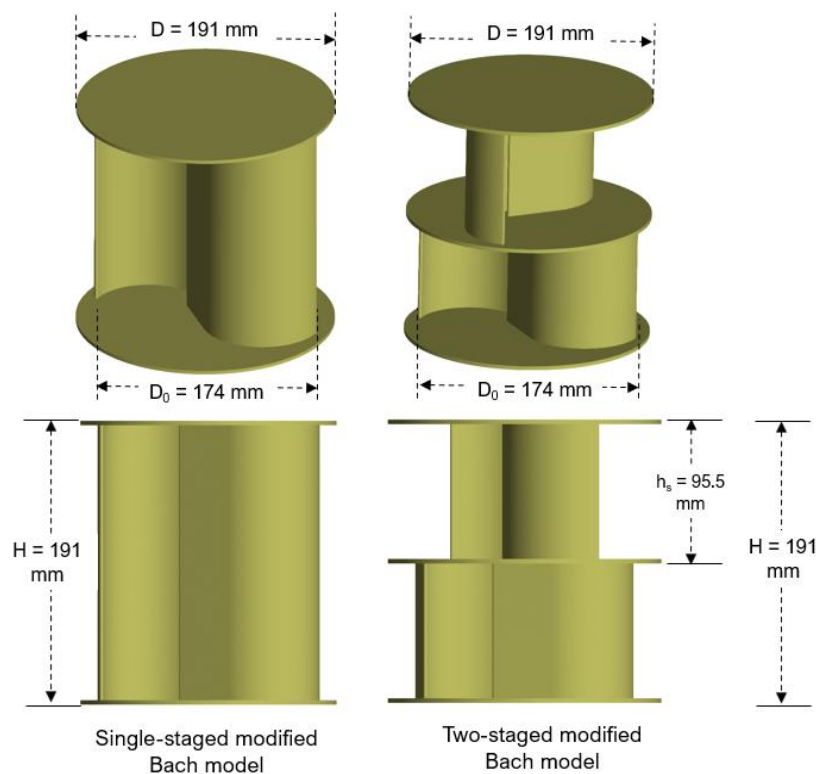


Fig. 5 Single-staged and two-staged modified Bach models used for the study

### 3.2 Computational domain

A 3D computational domain with the HKT model is created using the Flow-3D software. Two different zones namely- stationary and rotating are modeled. The stationary zone is characterized with a length of 2 m, width of 0.89 m and height of 1.4 m. The rotating zone is created as an enclosure around the turbine with fine mesh in order to capture the resulting forces and flow behavior around the turbine accurately. The length, width, and height for the rotating zone is specified with a value of 0.191 m each which is similar as the height and diameter of the overall turbine structure. The distance between the upstream boundary of the domain and the turbine centre is maintained at 2 times the diameter (2D) of the turbine. Similarly, a distance of 8D is allowed between the turbine and the downstream outlet boundary. The top and bottom boundaries of the domain are 3.5D apart from the turbine centre. Furthermore, the side boundaries measure 2.25D from the centre of the domain. These dimensions have been selected such that the resulting coefficients are not influenced by the effect of surrounding boundaries. To achieve the same, the specified dimensions for the turbine domain have been arrived upon after referring the HKT simulation studies from the published literature [30–32].

### 3.3 Boundary condition

The boundary conditions prescribed for the created computational domain are shown in Fig. 6. For the outer stationary zone, a velocity inlet (V) is provided at the upstream of the turbine and an inlet velocity value of 0.86 m/s which corresponds with the Re value of  $1.5 \times 10^5$  is specified. The flow is then designed to interact with the turbine before it flows to the outlet boundary (O). The outlet boundary facilitates smooth exit of the flow from the computational domain in a single direction thus avoiding backflow. To improve the stability of the simulations, symmetrical (S) boundary conditions are applied along the top and side boundaries of the stationary domain [33]. In symmetry conditions, the reflected flow after interaction with the moving turbine blades will have no influence on the resulting forces. Besides, it is assumed that the turbine operates at a proper depth such that it has no effect on the free surface of the flow.

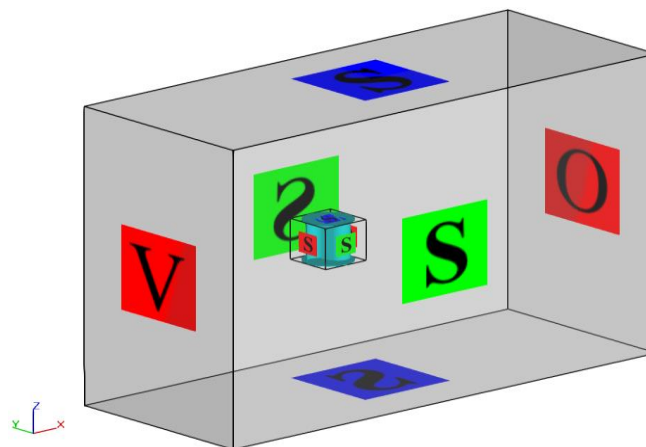


**Fig. 6** Schematic diagram of boundary condition

For the smaller enclosure around the turbine, symmetry conditions are prescribed for each of the walls to facilitate easy transition of flow from the stationary domain to the rotating domain. Furthermore, the symmetry condition will eliminate the discrepancies occurring in the resulting forces as well as flow behavior in the extremely turbulent flow around close vicinity of the turbine [34].

## 4 Validation and simulation

Two validation studies have been performed prior to the generation of final results regarding performance assessment of the two-staged modified Bach HKT. The first validation study is the mesh density analysis which is carried out to determine the optimal mesh size for the simulations. Determining the ideal value of mesh cells is very important to obtain a balance between accuracy as well as computational time. It is a well-acknowledged fact in the CFD industry that finer the mesh is, the more accurate will be the results. However, a downside that revolves around a more finer mesh than that required is the extensive computational time for running the entire simulation [35]. Hence, through the mesh density analysis, a good enough mesh cell size can be achieved that can provide acceptable results within a reasonable amount of time. To conduct the mesh density analysis, various sizes of mesh cells for both bigger and smaller domain are tested corresponding to different refinement levels. Each refinement level is then simulated for the flow velocity of 0.86 m/s. The torque coefficient ( $C_t$ ) is the parameter measured at the end of each simulation. The variations in the value of  $C_t$  are observed and the optimal value of mesh cell size for both the domains is selected when the variations in  $C_t$  become quite meagre or negligible.

The second validation study is conducted on the single-staged modified Bach HKT and the obtained results are compared with the experimental values of Roy and Saha. The validation of the designed 3D model is crucial for achieving reliability for the further study that involves comparison of single-staged and two-staged design. In addition, this validation will also provide benchmark measurements of the single-staged turbine for the comparison. The standard  $k - \epsilon$  turbulence model is employed for the simulation as it is superior to other available models in Flow-3D. It can be used to solve problems involving fluid flow in the vicinity of complex geometrical structures [36]. The standard  $k - \epsilon$  turbulence model uses wall functions based on the law of the wall to resolve the complex forces and flow interaction at sharp corners, straight and curved edges, such as those of the turbine blades [37]. The tip-speed ratio (TSR) is varied over a range of values from 0.158 to 1.145 and the performance parameters such as  $C_t$  and  $C_p$  are measured over the entire range of TSR.

After achieving the optimal mesh cell size and validation of the modeled geometry, the simulations are conducted for the two-staged modified Bach turbine for the Re of  $1.5 \times 10^5$ . The performance assessment parameters such as  $C_t$ ,  $C_t$ s and  $C_p$  are mainly focused during the study. Based on the results, comparisons are drawn between the single-staged and two-stage HKT. Also, to study the behavior of fluid pressure on the surface of the blades, pressure contours for both the turbine structures are studied.

## 5 Results and Discussion

### 5.1 Validation results

For the mesh density analysis, the cell size for the larger mesh block is varied from the highest value of 18 mm to the lowest value of 9 mm. Similarly for the smaller enclosure mesh block, the size varies from 8 mm to 2 mm as the highest and lowest values, respectively. As the nested mesh block method is used for meshing, it is important that the boundaries of smaller mesh block coincide with the corners of the mesh cells in the larger mesh block. In the given Fig. 7, we can clearly see that the corners of smaller mesh block coinciding with the cells of larger block and the same is maintained at each of the corners of the smaller 3D mesh domain.

Table 2 shows the finding of the mesh density analysis. It can be observed that the value of  $C_t$  changes with the increasing refinement levels or the decreasing mesh cell sizes in both mesh blocks. A notable difference can be observed between the  $C_t$  values of the first five refinement levels. After refinement level 5, a negligible difference was achieved in the results. Here, it can be said that the further decrease in mesh size has no influence on the output parameter and a level of stability has been achieved. Further decreasing the mesh cell size makes no difference to the result but only increases the simulation time for the solver. Hence, the refinement level 5 where the mesh cell size for bigger and smaller mesh block is 10 mm and 3 mm, respectively, is ideal for carrying out the simulation for the remainder of the study. The chosen mesh domain has a total number of mesh cells equaling  $2.43 \times 10^6$ .

For the second part of validation, the results obtained for the single-stage modified Bach HKT have been compared with the published experimental results of Roy & Saha [26]. The comparison between

the present simulation data and published experimental results is shown in Fig. 8 and 9. Fig. 8 shows the comparison for the parameter of  $C_t$ . Meanwhile, Fig. 9 illustrates the trend between the experimental and CFD results for  $C_p$ . Roy and Saha had achieved a peak  $C_p$  value of 0.280 at the TSR of 0.767. For the CFD results as well, a maximum  $C_p$  value of 0.298 occurs at the same TSR of 0.767. Among the different values achieved for  $C_t$  over the range of varied TSR, the one which corresponds with the TSR where the  $C_p$  value is maximum is considered to be the most important. The  $C_t$  value achieved during the experiments at the TSR of 0.767 was 0.364. Whereas from the CFD results, a value of 0.385 was achieved at the TSR of 0.767. It can be observed that, the simulated results demonstrated a similar trend and magnitude like the published results. Henceforth, the adopted methodology can be considered as reliable and acceptable to proceed with the further testing of the two-staged modified Bach turbine.

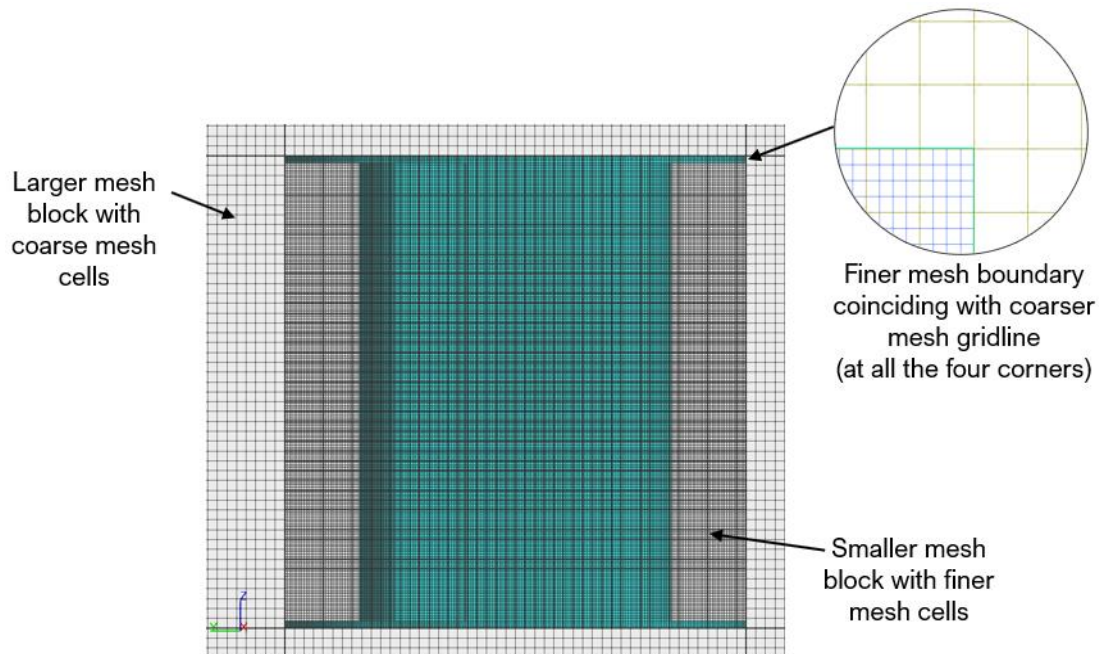
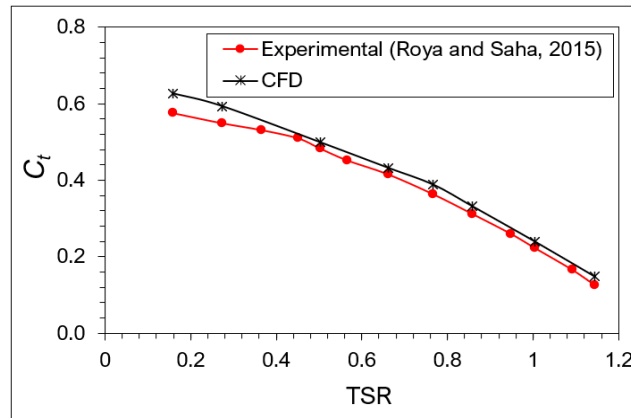


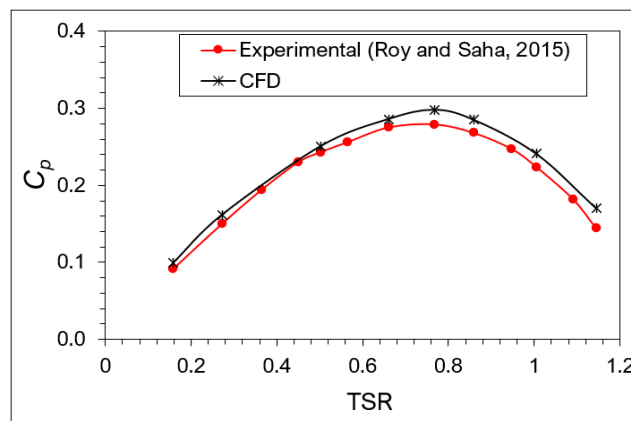
Fig. 7 Mesh block size

Table 2 Mesh density analysis finding

Refinement level	No. of mesh cells	Mesh cell size		$C_t$
		Bigger mesh block (mm)	Smaller mesh block (mm)	
1	$4.08 \times 10^5$	18	8	0.3
2	$6.75 \times 10^5$	15	7	0.38
3	$1.10 \times 10^6$	13	5.5	0.44
4	$1.17 \times 10^6$	13	4	0.39
5	<b><math>2.43 \times 10^6</math></b>	<b>10</b>	<b>3</b>	<b>0.43</b>
6	$2.62 \times 10^6$	10	2.5	0.43
7	$3.97 \times 10^6$	9	2	0.42



**Fig. 8** Graph of  $C_t$  experimental and CFD



**Fig. 9** Graph of  $C_p$  experimental and CFD

### 5.2 Comparison of the single-staged and two-staged modified Bach HKT

After validation and completion of simulations for the single-staged HKT, the two-staged modified Bach HKT is studied. Fig. 10 and 11 shows the performance comparison of  $C_t$  and  $C_p$  between the single-staged and two-staged HKT, respectively, for the TSR intervals from 0.158-1.145. The value of  $C_t$  for single-staged HKT is highest at the lowest TSR and can be observed to decrease gradually until it reaches the TSR value of 1.145. The peak  $C_t$  of 0.627 is recorded for the single-staged HKT at the TSR of 0.158. The  $C_t$  for two-staged HKT shows a similar trend where it decreases with the increment in TSR. However, a slight increase at 0.503 TSR is measured after which the  $C_t$  value continues to descend. For the two-staged HKT, the maximum  $C_t$  recorded is 0.551 at the TSR of 0.627.

Meanwhile, it is observed that the  $C_p$  for both the HKTs is lowest at the TSR of 0.158. A rise in the  $C_p$  is evident with the increasing TSR value and reaches a maximum point at the TSR of 0.767. After reaching the peak value, a further downward trend is visible. Overall, the calculated values show a similar bell curve trend in case of both the HKTs. As compared to the maximum  $C_p$  of 0.298 recorded for the single-staged HKT, a value of 0.322 is measured for the two-staged modified Bach HKT. This demonstrates that the increment in the number of stage results in an improvement in the efficiency value by 8%. Similarly, a relatively greater  $C_t$  by 9% is achieved for the two-staged modified Bach turbine.

The variations in static torque coefficient ( $C_{ts}$ ) for both the single and two-staged modified Bach HKT can be observed in Fig. 12. The  $C_{ts}$  values are calculated by fixing the HKTs at a static angular position and allowing the fluid flow through the turbines. To determine the point at which the maximum  $C_{ts}$  occurs is very crucial to identify the ideal starting angle of an HKT which will eventually improve its starting performance.

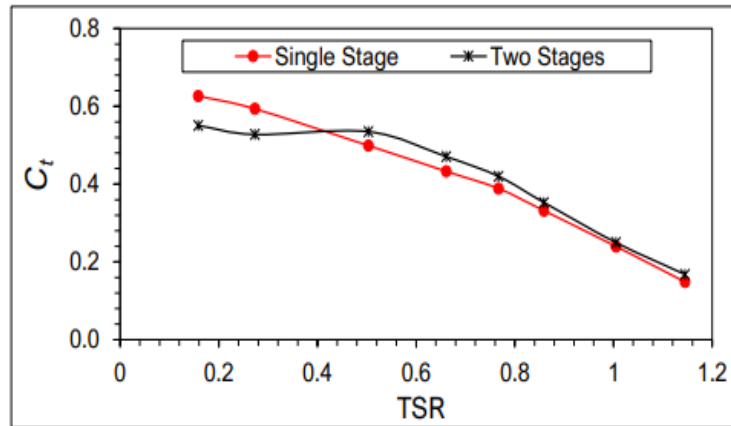


**Fig. 10** TSR vs  $C_t$  for single-staged and two stages modified Bach HKT

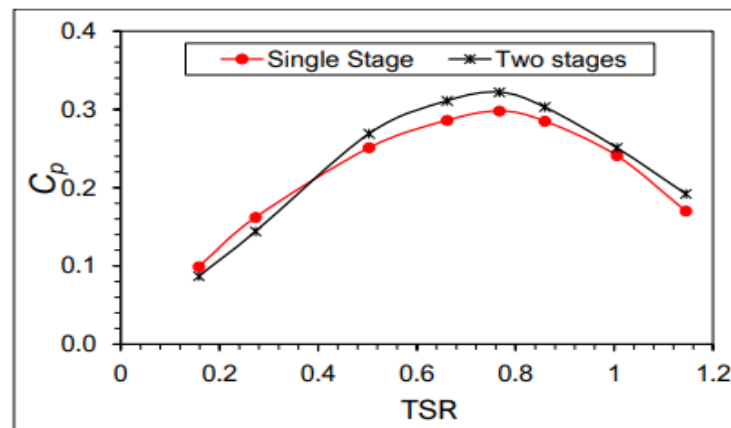


**Fig 11** TSR vs  $C_p$  for single and two stages

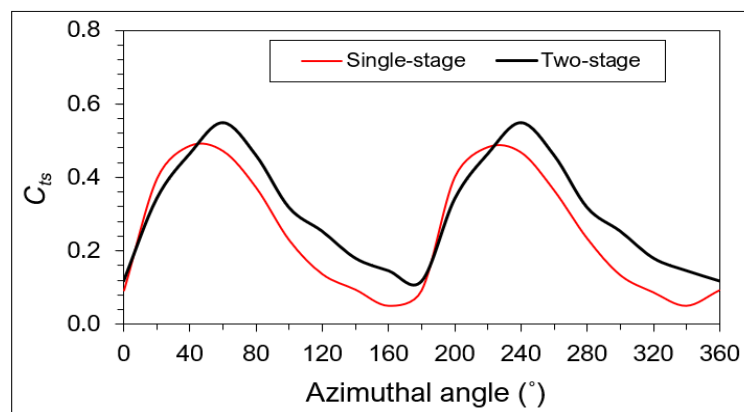


**Fig. 12** Static torque for single stage and two stages

At  $0^\circ$  angle, the two-staged HKT is noticed to have a higher torque than the single-staged. Two peaks in the trend occur for both the turbines. For the single-staged HKT, the peaks occur at  $40^\circ$  and  $220^\circ$ , whereas for the two-staged turbine, the peaks occur at  $60^\circ$  and  $240^\circ$ . The maximum  $C_{ts}$  achieved for the single staged HKT over the entire rotation is 0.464 which occurs at both the peak points. For two-staged HKT, the maximum value is 0.548. It can be noticed that the trend is repeated over the range of  $0^\circ$  to  $180^\circ$  since the turbine returns to the same angular position after the  $180^\circ$  rotation. The lowest value for the two-staged modified Bach HKT occurs at  $0^\circ$ ,  $180^\circ$  and  $360^\circ$ . This can be understood since at these orientations, the lowest swept area of the blades is exposed towards the incoming flow resulting in less magnitude of static torque generated. As the turbine starts to rotate in clockwise, a

greater area is exposed and the greater fluid force on the turbine blades leads to a greater generation of static torque. Meanwhile, as the blade turns towards 360° position, less area is exposed to the flow once again and minimum torque is observed.

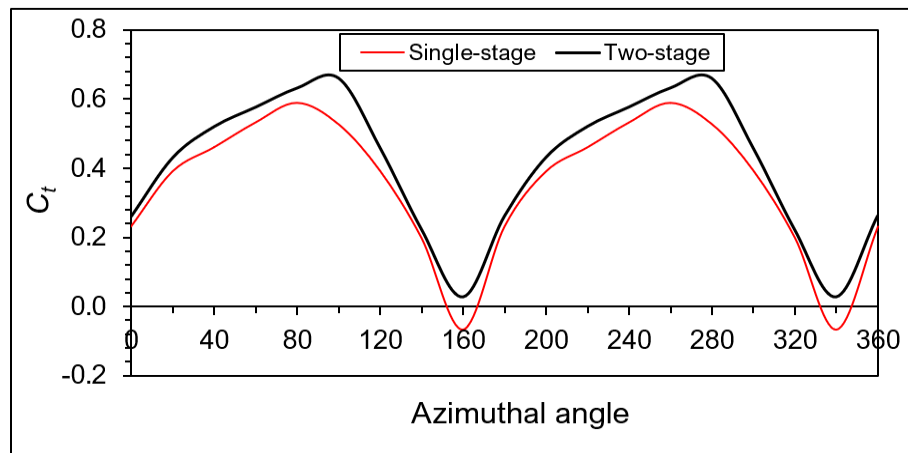


**Fig. 13** Dynamic torque for single stage and two stages

Unlike the static torque, the dynamic torque generated about the axis of the turbine results in its rotation. For both the turbines, the readings for torque are measured over the last 12 blade rotations at the TSR of 0.767 since both the designs demonstrate their most efficient performance at this TSR. The average  $C_t$  values at various azimuthal angles for both the single-stage and two-stage HKTs are plotted in Fig. 13. It can be observed that there is a negative torque recorded for single-staged at 160° and 340°. This can be explained by the fact that for the designs based on Savonius concept, negative torque occurs when the complete swept area of the returning blade is exposed to the incoming flow. The maximum  $C_t$  of 0.59 occurs for the single staged turbine at the azimuthal angle of 80° and 260°. In case of two-staged turbine, a highest  $C_t$  value of 0.659 which is greater than the maximum  $C_t$  of single-staged by 11% occurs at angles of 100° and 280°. Similar to that of  $C_{ts}$ , a periodic wave trend is visible for both the HKT models over the azimuthal angle range from 0° to 360°.

However, an important observation that contributes significantly towards the improved performance of two-staged modified Bach HKT is the elimination of negative torque. In contrast to the single-staged HKT, no presence of negative torque is evident over the entire turbine rotation. The reason for the same is that unlike in the case of the single-staged HKT, the two-staged turbine is never in an azimuthal position where the returning blade is the only thing exposed to the flow. As a result of the two-staged arrangement, the point where the returning blade is exposed to the flow coincides with the orientation where the advancing bucket of the other stage is exposed to the flow. Hence, the negative torque generated on the returning blade of one stage is balanced with the positive torque generated on the advancing blade of the other stage. Although it is true that the overall torque generated at such an orientation towards incoming flow will be lower, as observed at angles 160° and 340° for the two-staged HKT, it is not negative as in the case of single-staged HKT.

Fig. 14 demonstrates the pressure contours of the single and two-staged HKT during operation. As the velocity is low, the pressure on the turbine is expected to become greater. It can be seen that the concave surface (inner curve blade) yields a higher pressure compared to the convex surface (outer curve blade). This difference in pressure between the two sections of the blade effects the rotation of blade in clockwise direction.

### 5.3 Economic aspects

The overall efficiency of the entire turbine setup,  $\eta_0$ , and the power output from the single-staged and two-staged HKT is calculated using the following equation:

$$\eta_0 = \eta_T \times \eta_G \times \eta_{TS} \quad (1)$$

where  $\eta_T$ ,  $\eta_G$  and  $\eta_{TS}$  are the efficiency values corresponding to the turbine, electric generator, and transmissions and storage system, respectively.

Furthermore, the power output of the HKT is given as the power available multiplied with the overall efficiency of the turbine setup and is given as:

$$\text{Power output of HKT} = 0.5\rho AV^3 \times \eta_0 \quad (2)$$

where  $\rho$  is the fluid density,  $A$  is the blade swept area, and  $V$  is the fluid velocity.

To calculate the payback period, it is assumed that the capital and maintenance cost to be 400 USD and 100 USD after referring to. Thus, the payback period for the two-staged modified Bach turbine is calculated by the following equation [26]:

$$\text{Payback period} = \frac{\text{Total Cost}}{\text{Power cost per kWh} \times \text{Power output in kWh}} \quad (3)$$

$$= \frac{400 + 100}{1.14 \times 0.35} = 1253.13 \text{ days} = 3.4 \text{ years}$$

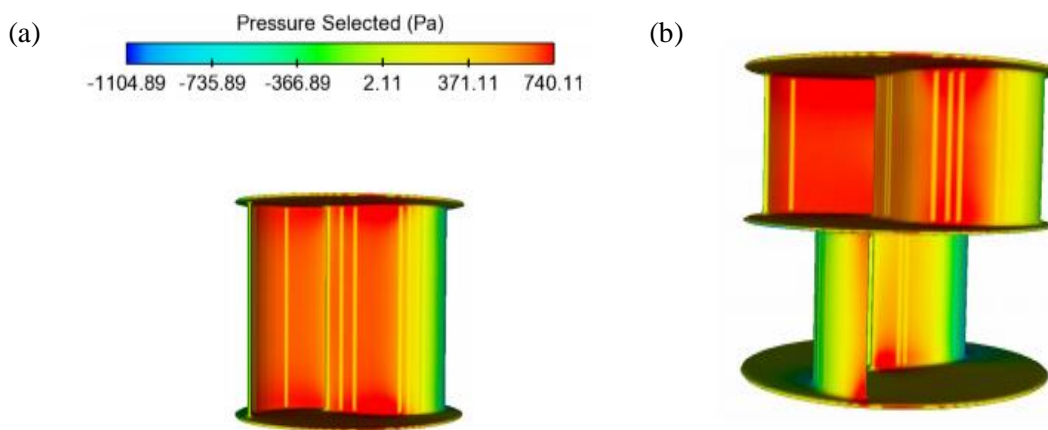


**Fig. 14** (a) Pressure contour for single-staged (b) Pressure contour for two-staged

**Table 3** Economical aspects for single stage and two stages

Parameters	Single-Staged HKT	Two-staged HKT
Turbine efficiency, $\eta_T$	30%	32.2%
Generator efficiency, $\eta_G$	80%	80%
Transmission-storage efficiency, $\eta_{TS}$	70%	70%
Overall efficiency of turbine, $\eta_0$	16.8%	18.0%
Available power in the wind, $W$	264.2	264.2
Power output	44.4W	47.6 W
Power output in kWh per day	1.07	1.14
Power cost per kWh	0.35USD	0.35USD
Turbine capital cost	400 USD	400 USD
Maintenance cost	100 USD	100 USD
Payback Period, years	3.7	3.4

## 6 Conclusion

The study aimed at achieving an optimized design of hydrokinetic turbine that is suitable for low-velocity river applications. For this study, the modified Bach Savonius turbine was selected as the base model owing to its better performance reported in the literature as compared to the conventional Savonius. The modified Bach turbine was initially modeled and validated with the existing experimental results using 3D CFD simulations. Later, the optimization technique of multi-staging was employed, and a two-staged HKT design was designed. The performance evaluation of the modified HKT design was conducted at the similar Reynold's number of  $1.5 \times 10^5$ . From the comparison of obtained results, it was found that the torque extraction capacity of modified two stages Bach model was improved by 9%. The better torque extraction subsequently enhanced the  $C_p$  value by 8.1%. Also, it was observed that the two-staged turbine showed lower torque fluctuations which implies that the optimized turbine will suffer from less vibration forces. Taking into consideration the low-flow velocity of 0.86 m/s used for the simulations, the reported efficiency of 32.2% can be considered as notably upgraded. Furthermore, comparisons were drawn on the economic aspects for both the single-staged and the two-staged HKT. Owing to the improved efficiency for the two stages turbine a lower payback period of 3.4 years for the investments was calculated as compared to the 3.7-year period for the single-stage turbine. The main objective of this research is to increase the performance of existing HKT for low-speed river current by modifying the existing HKT.

## Declaration of Conflict of Interest

The authors declared that there is no conflict of interest with any other party on the publication of the current work.

## ORCID

Ng Cheng Yee  <https://orcid.org/0000-0002-6915-5647>

## References

- [1] P. Yatim, M.N. Mamat, S.H. Mohamad-Zailani, S. Ramlee, Energy policy shifts towards sustainable energy future for Malaysia, *Clean Technologies and Environmental Policy* 18 (2016) 1685–1695. <https://doi.org/10.1007/s10098-016-1151-x>.
- [2] International Energy Agency. *Global Energy & CO2 Status Report*, Paris, 2019.
- [3] B. Mayor, I. Rodríguez-Muñoz, F. Villarroya, E. Montero, E. López-Gunn, The role of large and small scale hydropower for energy and water security in the Spanish Duero basin, *Sustainability* 9(10) (2017) 1807. <https://doi.org/10.3390/su9101807>.
- [4] A.V. Nekrasov, D.A. Romanenkov, Impact of tidal power dams upon tides and environmental conditions in the Sea of Okhotsk, *Continental Shelf Research*, 30 (2010) 538–552. <https://doi.org/10.1016/j.csr.2009.06.005>.
- [5] A.N. Gorban', A.M. Gorlov, V.M. Silant'ev, Limits of the turbine efficiency for free fluid flow, *Journal of Energy Resources Technology* 123 (2001) 311–317. <https://doi.org/10.1115/1.1414137>.
- [6] N.D. Laws, B.P. Epps, Hydrokinetic energy conversion: Technology, research, and outlook, *Renewable & Sustainable Energy Reviews* 57 (2016) 1245–1259. <https://doi.org/10.1016/j.rser.2015.12.189>.
- [7] M. Badrul Salleh, N.M. Kamaruddin, Z. Mohamed-Kassim, Savonius hydrokinetic turbines for a sustainable river-based energy extraction: A review of the technology and potential applications in Malaysia, *Sustainable Energy Technologies and Assessments* 36 (2019) 100554. <https://doi.org/10.1016/j.seta.2019.100554>.
- [8] P.K. Talukdar, V. Kulkarni, U.K. Saha, Performance estimation of Savonius wind and Savonius hydrokinetic turbines under identical power input, *Journal of Renewable and Sustainable Energy* 10 (2018) 064704. <https://doi.org/10.1063/1.5054075>.
- [9] N.R. Maldar, C.Y. Ng CY, E. Oguz, A review of the optimization studies for Savonius turbine considering hydrokinetic applications, *Energy Conversion and Management* 226 (2020) 113495. <https://doi.org/10.1016/j.enconman.2020.113495>.
- [10] A. Kumar, R.P. Saini, Performance analysis of a Savonius hydrokinetic turbine having twisted blades, *Renewable Energy* 108 (2017) 502–522. <https://doi.org/10.1016/j.renene.2017.03.006>.

- [11] T. Burton, N. Jenkins, B. Ervin, D. Sharpe, M. Graham, Wind Energy Handbook, 3<sup>rd</sup> ed.. Wiley Online Library, 2021.
- [12] J. VanZwieten, W. McAnally, J. Ahmad, T. Davis, J. Martin, M. Bevelhimer, A. Cribbs, R. Lippert, T. Hudon, M. Trudeau, In-Stream hydrokinetic power: Review and appraisal, Journal of Energy Engineering 141 (2015) 04014024. [https://doi.org/10.1061/\(asce\)ey.1943-7897.0000197](https://doi.org/10.1061/(asce)ey.1943-7897.0000197).
- [13] I.B. Alit, R. Sutanto, I.M. Mara, M. Mirmanto, Effect of concentrator, blade diameter and blade number on the Savonius wind turbine performance, Asian Journal of Applied Sciences 5(2) (2017) 343–351. <https://doi.org/10.24203/ajas.v5i2.4610>.
- [14] J.P. Abraham, B.D. Plourde, G.S. Mowry, W.J. Minkowycz, E.M. Sparrow, Summary of Savonius wind turbine development and future applications for small-scale power generation, Journal of Renewable Sustainable Energy 4(4) (2012) 042703. <https://doi.org/10.1063/1.4747822>.
- [15] D. Mahesa Prabowoputra, S. Hadi, J.M. Sohn, A.R. Prabowo, The effect of multi-stage modification on the performance of Savonius water turbines under the horizontal axis condition, Open Engineering 10 (2020) 793–803. <https://doi.org/10.1515/eng-2020-0085>.
- [16] M. Nakajima, S. Iio, T. Ikeda, Performance of double-step Savonius rotor for environmentally friendly hydraulic turbine, Journal of Fluid Science and Technology 3 (2008) 410–419. <https://doi.org/10.1299/jfst.3.410>.
- [17] M.N.I. Khan, M. Tariq Iqbal, M. Hinchey, V. Masek, Performance of Savonius rotor as a water current turbine, The Journal of Ocean technology 4 (2009) 71–83.
- [18] J.L. Menet, A double-step Savonius rotor for local production of electricity: A design study, Renewable Energy 29 (2004) 1843–1862. <https://doi.org/10.1016/j.renene.2004.02.011>.
- [19] U.K. Saha, S. Thotla, D. Maity, Optimum design configuration of Savonius rotor through wind tunnel experiments, Journal of Wind Engineering and Industrial Aerodynamics 96 (2008) 1359–1375. <https://doi.org/10.1016/j.jweia.2008.03.005>.
- [20] K. Golecha, T.I. Eldho, S.V. Prabhu, Influence of the deflector plate on the performance of modified Savonius water turbine, Applied Energy 88 (2011) 3207–3217. <https://doi.org/10.1016/j.apenergy.2011.03.025>.
- [21] O.B. Yaakob, D.T. Suprayogi, M.P. Abdul Ghani, K.B. Tawi, Experimental studies on savonius-type vertical axis turbine for low marine current velocity. International Journal of Engineering Transaction A: Basics 26 (2013) 91–98. <https://doi.org/10.5829/idosi.ije.2013.26.01a.12>.
- [22] K.K. Sharma, R. Gupta, A. Biswas, Performance measurement of a two-stage two-bladed Savonius rotor, International Journal of Renewable Energy Research 4 (2014) 115–121.
- [23] S. Frikha, Z. Driss, E. Ayadi, Z. Masmoudi, M.S. Abid, Numerical and experimental characterization of multi-stage Savonius rotors, Energy 114 (2016) 382–404. <https://doi.org/10.1016/j.energy.2016.08.017>.
- [24] L.B. Kothe, S.V. Möller, A.P. Petry, Numerical and experimental study of a helical Savonius wind turbine and a comparison with a two-stage Savonius turbine, Renewable Energy 148 (2020) 627–638. <https://doi.org/10.1016/j.renene.2019.10.151>.
- [25] E. Kerikou, D. Thévenin, Optimal shape of thick blades for a hydraulic Savonius turbine, Renewable Energy 134 (2019) 629–638. <https://doi.org/10.1016/j.renene.2018.11.037>.
- [26] S. Roy, U.K. Saha, Wind tunnel experiments of a newly developed two-bladed Savonius-style wind turbine, Applied Energy 137 (2015) 117–125. <https://doi.org/10.1016/j.apenergy.2014.10.022>.
- [27] J. Chen, L. Chen, L. Nie, H. Xu, Y. Mo, C. Wang, Experimental study of two-stage Savonius rotors with different gap ratios and phase shift angles, Journal of Renewable and Sustainable Energy 8 (2016) 063302. <https://doi.org/10.1063/1.4966706>.
- [28] A. Kumar, R.P. Saini, Numerical investigations on single stage and multi-stage twisted Savonius hydrokinetic turbine, Proceeding of 6<sup>th</sup> International and 43<sup>rd</sup> National Conference Fluid Mechanics and Fluid Power, December 15-17, 2016, MNNITA, Allahabad, UP, India FMFP2016 2016:1–3.
- [29] N.H. Mahmoud, A.A. El-Haroun, E. Wahba, M.H. Nasef, An experimental study on improvement of Savonius rotor performance, Alexandria Engineering Journal 51 (2012) 19–25. <https://doi.org/10.1016/j.aej.2012.07.003>.
- [30] X. Li, M. Li, S.J. McLelland, L.B. Jordan, S.M. Simmons, L.O. Amoudry, R. Ramirez-Mendoza, P. D. Thorne, Modelling tidal stream turbines in a three-dimensional wave-current fully coupled oceanographic model, Renewable Energy 114 (2017) 297–307. <https://doi.org/10.1016/j.renene.2017.02.033>.
- [31] C. Cardona-Mancilla, R.J.S. Del, D. Hincapié-Zuluaga, E. Chica, A numerical simulation of horizontal axis hydrokinetic turbine with and without augmented diffuser, International Journal of Renewable Energy Research 8 (2018) 1833–1839.
- [32] N. Osbourne, D. Groulx, I. Penesis, Three dimensional simulation of a horizontal axis tidal turbine comparison with experimental results, 2<sup>nd</sup> Asian Wave Tidal Energy Conference, 2014.

- [33] W. Tian, Z. Mao, H. Ding, Design, test and numerical simulation of a low-speed horizontal axis hydrokinetic turbine, *International Journal of Naval Architecture and Ocean Engineering* 10 (2018) 782–793. <https://doi.org/10.1016/j.ijnaoe.2017.10.006>.
- [34] A. Rezaeiha, I. Kalkman, B. Blocken, CFD simulation of a vertical axis wind turbine operating at a moderate tip speed ratio: Guidelines for minimum domain size and azimuthal increment, *Renewable Energy* 104 (2017) 373–385. <https://doi.org/10.1016/j.renene.2017.02.006>.
- [35] N. Maldar, C.Y. Ng, A. Fitriadhy, H.S. Kang, Numerical investigation of an efficient blade design for a flow driven horizontal axis marine current turbine, *Lecture Notes in Civil Engineering* 132 (2021) 241–248. [https://doi.org/10.1007/978-981-33-6311-3\\_28](https://doi.org/10.1007/978-981-33-6311-3_28).
- [36] N.R. Maldar, C.Y. Ng, L.W. Ean, E. Oguz, A. Fitriadhy, H.S. Kang, A comparative study on the performance of a horizontal axis ocean current turbine considering deflector and operating depths, *Sustainability* 12 (2020) 3333. <https://doi.org/10.3390/SU12083333>.
- [37] N.K. Sarma, A. Biswas, R.D. Misra, Experimental and computational evaluation of Savonius hydrokinetic turbine for low velocity condition with comparison to Savonius wind turbine at the same input power, *Energy Conversion and Management* 83 (2014) 88–98. <https://doi.org/10.1016/j.enconman.2014.03.070>.